Regular Article

PHYSICAL CHEMISTRY RESEARCH
Published by the
Iranian Chemical Society
www.physchemres.org
info@physchemres.org

Phys. Chem. Res., Vol. 12, No. 1, 205-217, March 2024
DOI: 10.22036/pcr.2023.390388.2314

Exploring the Potential of Quantum Chemical Calculations for Synthesized Quinazoline Derivatives as Superior Corrosion Inhibitors in Acidic Environment

O.H.R. Al-Jeilawi*, H.N. Al-Ani, A. Al-Zahra and K.T.A. AL-Sultani
Department of Chemistry, College of Sciences, University of Baghdad, Baghdad, Iraq
(Received 19 March 2023, Accepted 20 June 2023)

Hydrochloric acid (HCl) is a substance that is frequently utilized in industrial operations for important tasks such as chemical cleaning and pickling metallic surfaces. The main issue with using this compound is that metallic surfaces rust, which leads to corrosion becoming a permanent issue. Corrosion inhibitors are an excellent solution to this problem since they may reduce the corrosion phenomena and increase the service life of metallic structures and equipment. Therefore, the corrosion inhibition ability of three newly synthesized quinazoline derivatives namely, 3-allyl-2-(propylthio) quinazolin-4(3H)-one) (APQ), (3-allyl-2-(allylthio) quinazolin-4(3H)-one) (AAQ), (3-allyl-2-(Prop-2-yn-1-ylthio) Quinazolin-4(3H)-one) (AYQ) were theoretically determined and these compounds were characterized using Fourier Transform Infra-Red (FTIR) and ^{1}H and ^{13}C Nuclear Magnetic Resonance (NMR) spectroscopic. A series of quantum chemical properties of these derivatives: E_{HOMO}, E_{LUMO}, energy gap (ΔE), dipole moment (μ), hardness (η), softness (ϭ), absolute electronegativity (χ), fractions for electron transferred (ΔN), the ionization potential (I), (TE) and total energy were calculated. The obtained results of all quinazoline derivatives (APQ, AAQ, and AYQ) show almost the same corrosion inhibition with excellent efficiency. Density function theory (DFT) was used to investigate the relationship between the molecular structures and inhibitory efficacies of three quinazoline derivatives. The results of the analysis and measurement of E_{gap} values revealed that the compound AYQ had a modest E_{gap} of 4.999 eV and that strong values of E_{gap} suggest that it will be easier to remove one electron from the HOMO orbital and deposit it in the LUMO orbital. In contrast to APQ and AAQ, the AYQ was more readily adsorbed onto the surface of carbon steel due to its high reactivity, which increased its inhibitory effectiveness. According to the relationship CC > C=C > C-C, the efficacy of inhibition will occur.

Keywords: DFT, Quinazolinone derivatives, Corrosion inhibitor, Quantum chemistry, Theoretical predictions

INTRODUCTION

Due to the fact that iron materials, which are more vulnerable to being attacked in aggressive media, are the typically exposed metals in industrial environments, the necessity of carbon steel protection against corrosion in acidic solutions has expanded. Acid solutions are often employed in industrial procedures such as oil well acidification, petrochemical processes, acid pickling, acid cleaning, and acid de-scaling. These processes typically result in substantial metallic corrosion [1-4]. In order to increase oil output, petroleum oil wells are frequently acidified by injecting an 18% hydrochloric acid solution through N80 steel tubing. Due to the detrimental effects of corrosion on N80 tubing during this process, it is necessary to lessen the acid's severe attack on the tube and casing materials (steel), during the process of acidification, inhibitors are injected into the acid solution [5-8]. One of the most practical and easy ways to prevent metals from corroding, especially in acidic environments, is to utilize inhibitors. Organic corrosion inhibitors are molecules that interact with the metallic surface to form a protective coating that can slow down the oxidation process when introduced directly to an aggressive media like HCl. This mechanism is

*Corresponding author. E-mail: oday.organic@gmail.com

explained by certain structural characteristics that function as Lewis basic sites (n and Л-electrons) and interact with the alloy's constituent components to enable the adsorption of inhibitors on the metallic surface [9-11]. The most effective organic inhibitors are those that include triple bonds, electronegative groups, or have conjugated double bonds due to their nucleophilicity and capacity to bind the metal surface through interactions [12]. The inclusion of aromatic rings and heteroatoms like oxygen, sulfur, nitrogen, and phosphorus in the structure improves the effectiveness of these compounds' capacity to adsorb on metal surfaces and limit corrosion [13, 14]. The efficacy of these organic compounds' inhibition is significantly influenced by their planarity and projected surface area in addition to the number of heteroatoms [15]. Numerous quinazoline derivatives were explored for their ability to prevent corrosion in various harsh conditions. Fouda [16] employed a few variants of chlorophenyl and nitrophenyl quinazoline to prevent corrosion on carbon steel in a 2 M HCl solution. Al-tamimy [17] recognized the ability of 2-pentadecyl-quinazolinylthiourea to control corrosion in an acidic solution for carbon steel. Hash [18] examined the behavior of corrosion inhibition in an H_2SO_4 media while synthesizing three novel quinazoline derivatives. Recently, Rbaa [19] synthesized derivatives of the hydroxy quinazoline and showed how well they inhibited corrosion in HCl. In hydrochloric acid solutions, 3-cyclopropyl-3,4-dihydroquinoline-2(1H)-one was investigated by Abdelkarim *et al*. [20]. Kadhim has studied the properties of 2-methyl quinazoline-4(3H)-one that limits corrosion [21]. Two quinazoline derivative di-cationic surfactants were synthesized by Ozturk, who also investigated their corrosion inhibition behavior in acidic conditions [22]. In corrosion studies, the rate of corrosion can be effectively investigated using various electrochemical methods, including electrochemical impedance spectroscopy, electrochemical frequency modulation, and potentiodynamic polarization. These techniques provide valuable insights into the corrosion process and allow for the quantification of corrosion rates and the evaluation of corrosion inhibitors. Electrochemical impedance spectroscopy (EIS) is powerful tool that measures the impedance response of a corroding system as a function of frequency. By analyzing the impedance data, important parameters such as corrosion resistance, charge transfer resistance, and double-layer capacitance can be determined, providing valuable information about the corrosion behavior and the effectiveness of corrosion inhibitors. While Electrochemical frequency modulation (EFM) is another electrochemical technique used to investigate corrosion rates. It measures the change in frequency of an oscillating potential applied to the system, which is directly related to the corrosion rate. EFM offers advantages for example high sensitivity and the ability to provide real-time corrosion rate measurements [23-29].

However, Quantum chemical calculations (QCCs) are a potent tool for understanding the physicochemical aspects involved in the interactions between a metallic surface and an anticorrosive compound. It is commonly known from the literature that the inhibition efficiency of an organic molecule is significantly associated with its electronic structure. The utilization of these theoretical calculations in this context yields a number of electronic characteristics (Electronegativity, electron affinity, energy gaps, frontier orbital energies, ionization potential, etc.) that are connected with the effectiveness of inhibition on an organic molecule [30,31]. Thus, in the interest of identifying new corrosion inhibitors, we synthesized three organic molecules derived from quinazolinone (Fig. 1). That is to say, instead of using the experimental routes to examine the corrosion efficiencies of possible inhibitors (synthesized compounds), these routes are non-ecological and expensive, we applied QCCs to conduct some of the theoretical calculations and predictions to support and prove the corrosion efficiencies of synthesized compounds as possible inhibitors.

In light of the aforementioned observations, the objective of the current study is to synthesize three new quinazoline derivatives, namely 3-allyl-2-(propylthio) quinazolin-4(3H)-one) (APQ), (3-allyl-2-(allylthio) quinazolin-4(3H)-one) (AAQ), (3-allyl- 2-(Prop -2-yn -1-ylthio) Quinazolin-4(3H) -one) (AYQ) and characterized using Fourier Transform Infra-Red (FTIR) and ^{1}H and ^{13}C Nuclear Magnetic Resonance (NMR) spectroscopic. The corrosion efficiency of these compounds was then evaluated theoretically by QCCs.

EXPERIMENTAL

Materials

All the chemical compounds used in the current study were of analytical grades and purchased from Sigma-Aldrich.

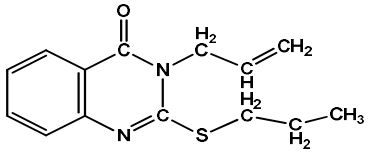

3-allyl-2-(propylthio)quinazolin-4(3*H*)-one

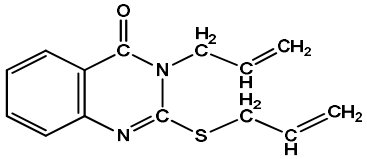

3-allyl-2-(allylthio)quinazolin-4(3*H*)-one

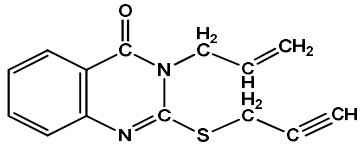

3-allyl-2-(prop-2-yn-1-ylthio)quinazolin-4(3*H*)-one

Fig. 1. The chemical structures of synthesized quinazoline derivatives (Corrosion inhibitors).

Apparatus

All solvents were supplied by commercial sources without additional decontamination. ^{1}H NMR and ^{13}C NMR spectra of compounds were obtained from (AV-400 MHz instrument, Bruker) using TMS as the internal standard. Thin layer chromatography (TLC, provided by Merck, coated on silica gel plate with 0.25 mm as a layer thickness) was used to check the purity of the compounds. The melting point of compounds was taken on the Electrothermal Programmable Digital Melting Point Apparatus (Scientific Fisher).

Synthesis of Inhibitors

Synthesis of 3-allyl-2-(propylthio)quinazolin-4(3H)-one) (1) [32]. A (5.0 g) of potassium thiocyanate (KNCS) was added to a 50 ml round bottom flask and dissolved in (20 ml) absolute ethanol while being stirred to aid in the dissolution process. Allyl bromide was then added, and the mixture was refluxed for an hour before the addition of anthranilic acid and triethyl amine, which was added three to four hours after the end of the reaction. The obtained precipitate was then submerged in Ice-cold water before filtering, washing, and drying. The precipitate was off-white; M. Wt. ($C_{11}H_{10}N_2OS$) = (218.3) g mol^{-1}; yield (70%); M.P. = (217-219) °C; FTIR. (K-Br): ν (=C-H) in 3045 cm^{-1}, ν (C-H) aromatic in 3015 cm^{-1}, ν (C-H) in 2939 cm^{-1}, ν (S-H) in 2488 cm^{-1}, ν to (C =O) in 1654 cm^{-1}, ν (C =C) in 1649 cm^{-1}, ν (C =N) in 1622 cm^{-1}, ν to (C = C) aromatic in 1533 cm^{-1}; ^{1}H NMR ($CDCl_3$): δ = 9.9 ppm. (1H, s, SH), δ is 3.98 ppm. (2H, s, CH_2), δ is 5.21,5.23 ppm. (2H, d, =CH_2), δ is 5.99 ppm. (1H, m, =CH-), δ = 7.11-8.18 ppm. (4H, m, H aromatic); ^{13}C NMR ($CDCl_3$): δ = 48.8 ppm. (CH_2), δ is 118.8 ppm. (=CH_2), δ is 125.04-130.67 ppm. (C Aromatic), δ 135.54 ppm. (CH=), δ = 138.29 ppm. (C=N), δ = 175.79 ppm. (C=O).

General procedure for the synthesis of three quinazoline derivatives (APQ, AAQ, and AYQ) [6]. For APQ, 2.18 g of the compound (1) was dissolved in 25 ml of absolute methanol followed by the addition of 5 ml of propyl chloride (0.1 mmol) and 0.1 g of KOH. The solution mixture was then refluxed for 3 h. and poured on ice, and filtered. A white precipitate was obtained and washed with distilled water several times. To this, 10 ml absolute methanol, 5 ml of allyl bromide, and 0.05 g of KOH were added, stirred for 30 min at room temperature and refluxed for 3 h. for AAQ. A white precipitate was obtained and washed with distilled water several times. To this, 10 ml absolute methanol, 5 ml of prop-2-yn-1-ylchloride, and 0.05 g of KOH were added, stirred for 30 minutes at room temperature and refluxed for 3 h. for AYQ. A brown precipitate was obtained and washed with distilled water several times. After each reaction, TLC was used to ensure the reaction gets complete. The recrystallization of APQ, AAQ, and AYQ was performed using ethanol. All the synthetic steps are illustrated in Fig. 2.

Synthesis of (3-allyl-2-(propylthio)quinazolin-4(3H)-one) (APQ). A white precipitate; M. Wt ($C_{14}H_{16}N_2OS$) = (260.35) g mol^{-1}; Yield = (60%); M.P. = (198-200) °C; FTIR (KBr): ν (=C-H) in 3078 cm^{-1}, ν (C-H) Aromatic in 3043 cm^{-1}, ν (C- H) in 2968 cm^{-1}, ν (C = O) in 1670 cm^{-1}, ν (C=C) in 1658 cm^{-1}, ν (C=N) in 1622 cm^{-1}, ν (C=C)

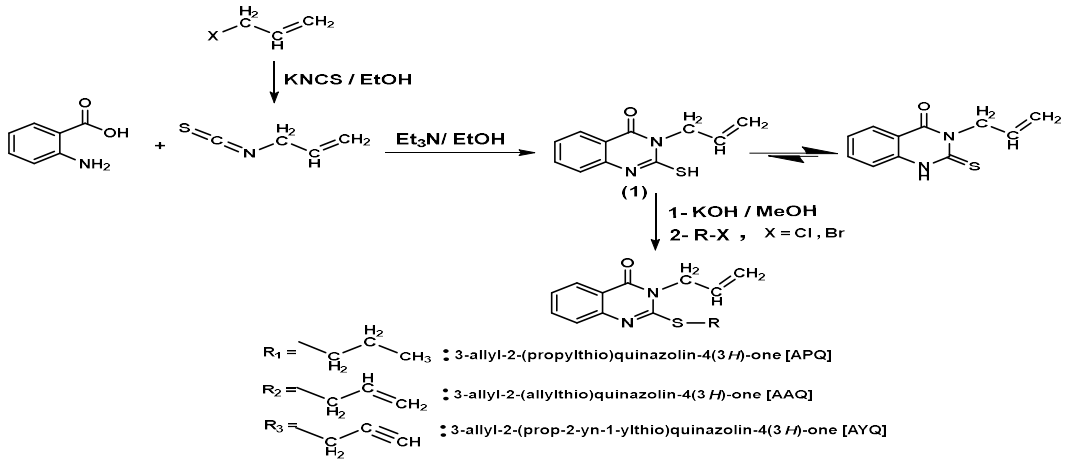

Fig. 2. The synthetic route of three corrosion inhibitors (APQ, AAQ, and AYQ).

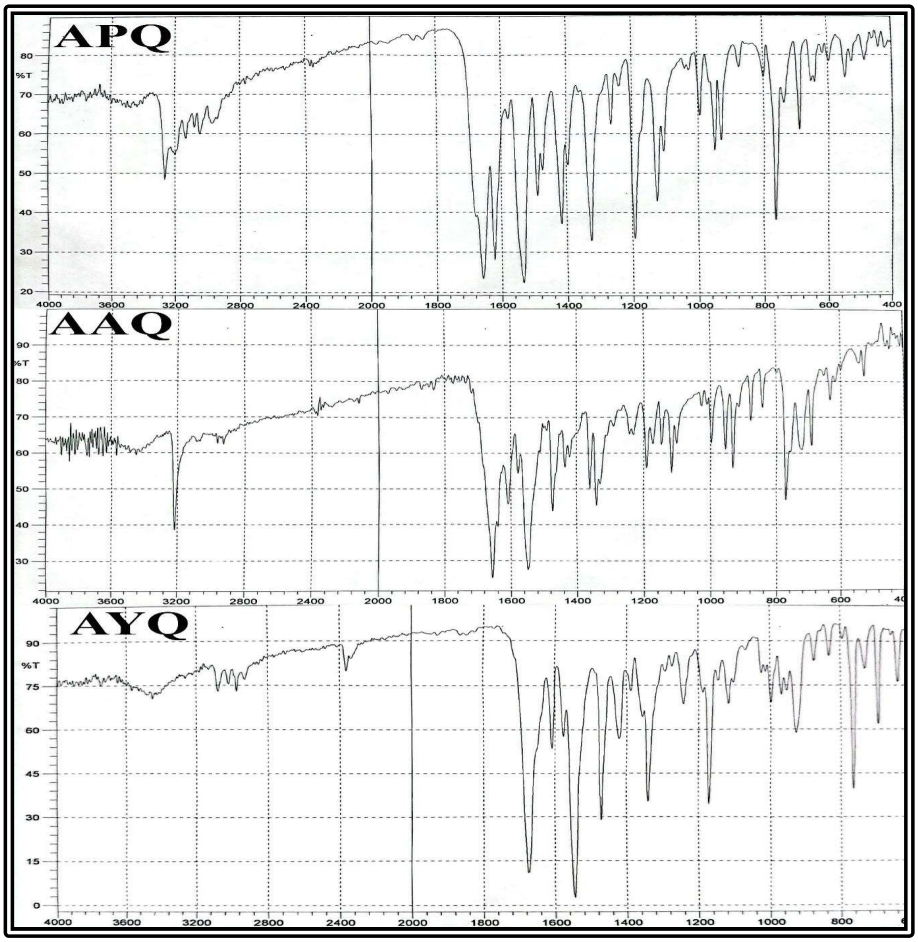

Fig. 3. The FTIR spectra for the prepared compounds (APQ, AAQ, AYQ) are presented as follows: Compound, APQ: The FTIR spectrum of APQ shows characteristic peaks at 1670 cm^{-1}, indicating the presence of carbonyl groups. Additionally, a peak at 3078 cm^{-1} suggests the presence of the =C-H group. The presence of aromatic rings is confirmed by the peaks observed in the region of 1500-1600 cm^{-1}. Compound AAQ: In the FTIR spectrum of AAQ, a prominent peak is observed at 1674 and 1640 cm^{-1}, indicating the presence of carbonyl group and C=C respectively. The presence of aromatic rings is evidenced by the peaks observed in the region of 1500-1600 cm^{-1}. Furthermore, a peak at 3016 cm^{-1} suggests the presence of aromatic C-H. Compound AYQ: The FTIR spectrum of AYQ exhibits a strong peak at 1548, 1636, and 1665 cm^{-1}, indicating the presence of aromatic C=C, C=C, and carbonyl group respectively. Peaks observed in the region of 1200-1400 cm^{-1} suggest the presence of aromatic rings. Additionally, a broad peak at 3215 cm^{-1} suggests the presence of C≡C.

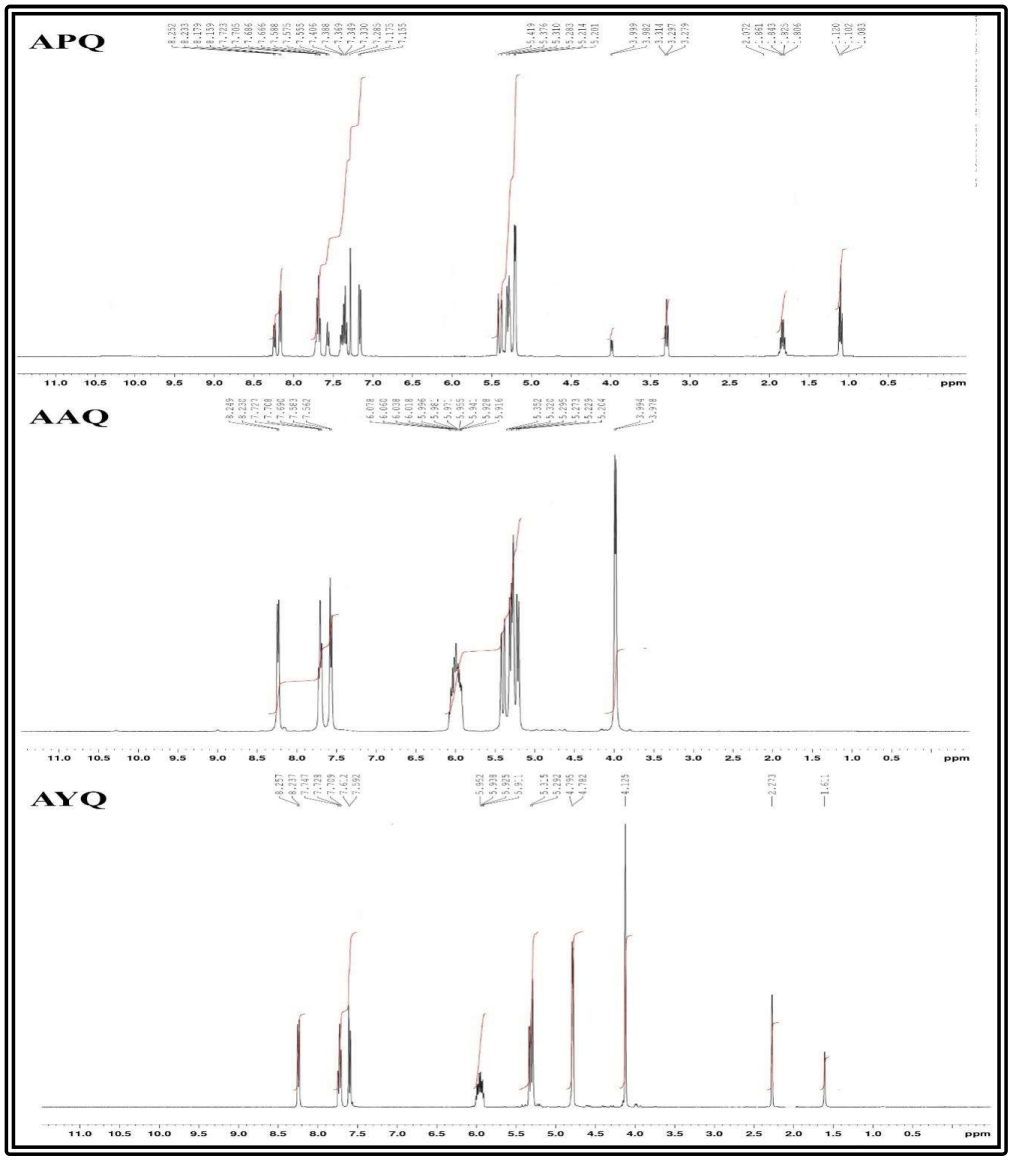

Fig. 4. H[1] NMR spectrum for prepared compounds (APQ, AAQ, AYQ).

aromatic in 1533 cm^{-1}; ^1H NMR. ($CDCl_3$): δ = 1.08 ppm. (3H, t, CH_3), δ = 1.65 ppm. (2H, m, CH_2), δ = 3.27 ppm. (2H, t, S-CH_2), 3.98 ppm. (2H, S, N-CH_2), 5.2,5.21 ppm. (2H, d, =CH_2), 5.99 ppm. (1H, m, =CH) δ = 7.55-8.15 ppm. (4H, m, H aromatic); ^{13}C NMR. (CDCl3): δ = 13.51 ppm. (CH_3), δ = 22.17 ppm. (CH_2), δ = 34.14 ppm. (=CH), δ = 46.23 ppm. (N-CH_2), δ = 118.36 ppm. (=CH_2), δ = 125.04-138.41 ppm. (C aromatic), δ = 134.29 ppm. (S-CH_2), δ = 159.38 ppm. (C=N), δ = 175.78 ppm. (C=O), as shown in Figs. 3-5.

Synthesis of (3-allyl-2-(allylthio)quinazolin-4(3H)-one) (AAQ). A white precipitate; M. Wt. ($C_{14}H_{14}N_2OS$) = (258.34) g mol^{-1}; yield (75%); M.P. = (54-56) °C; FTIR (KBr): ν (=C- H) in 3076 cm^{-1}, ν (C-H) aromatic at 3016 cm^{-1}, ν (C-H) at 2972 cm^{-1}, ν (C = O) in 1674 cm^{-1}, ν (C=C) in 1670 cm^{-1}, ν (C=N) in 1608 cm^{-1}, ν (C = C) aromatic in 1544 cm^{-1}; ^1H NMR. (CDCl3): δ. 3.97 ppm. (2H, d, S-CH_2), δ = 3.99 ppm. (2H, d, N-CH_2), δ = 5.20-5.29 ppm. (2H, d, =CH_2), 5.91-6.01 ppm. (1H, m, =CH), δ = 7.56-8.23 ppm. (4H, m, H Aromatic); ^{13}C NMR. (CDCl3): δ = 35.03 ppm. (=CH), δ = 46.25 ppm. (N- CH_2), δ = 118.52-118.94 ppm. (=CH_2), δ = 130.86 ppm (=CH), δ = 132.59 ppm. (S-CH_2), δ = 126.10-147.44 ppm. (C aromatic),

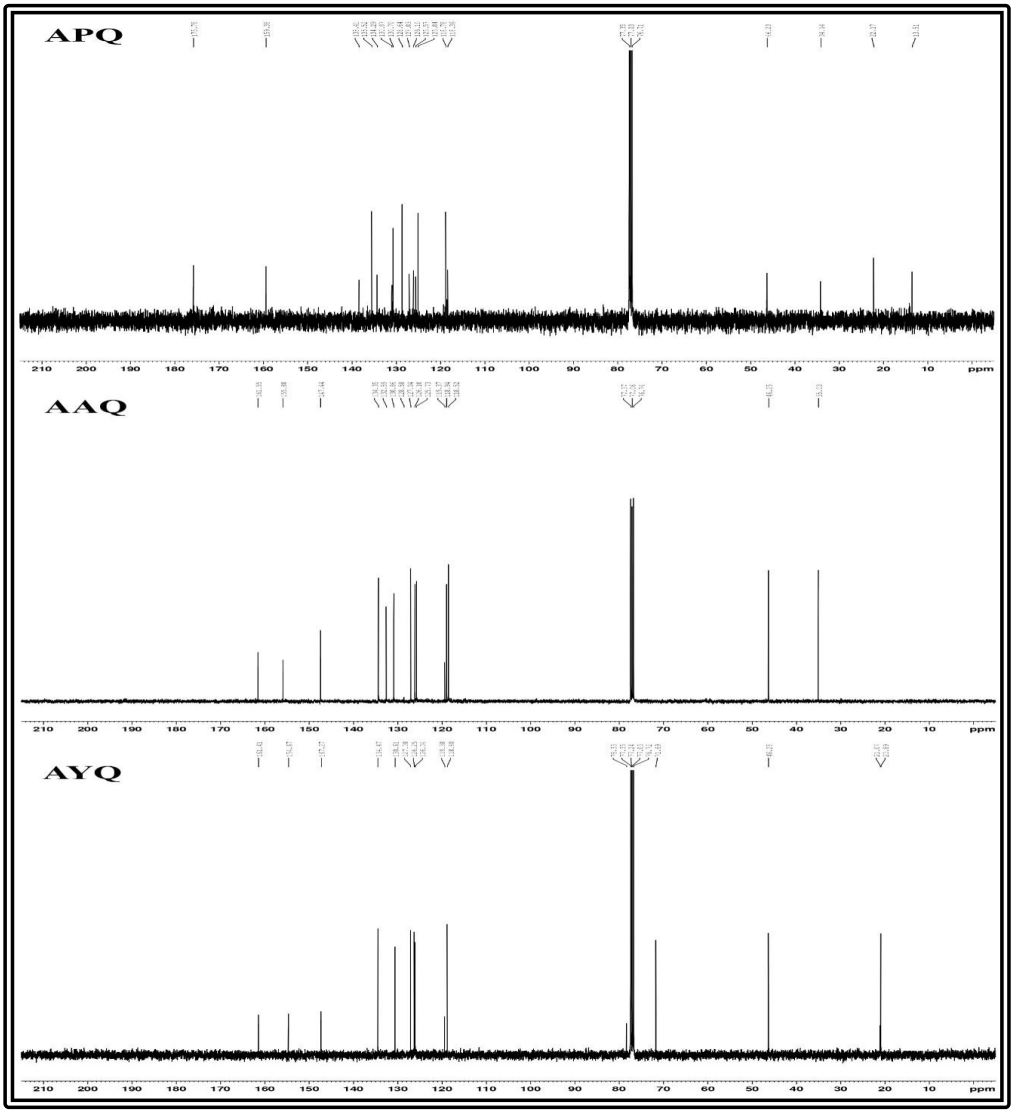

δ = 155.88 ppm. (C=N), δ =161.55 ppm. (C=O), as shown in Figs. 3-5.

Synthesis for (3-Allyl-2-(Prop-2-Yn-1-ylthio) quinazolin-4(3H)-one) (AYQ). A brown precipitate; M. Wt. ($C_{14}H_{12}N_2OS$) = (256.33) g mol^{-1}; yield (91%); M. P. = 108-110 °C; FTIR (KBr): ν. (≡C- H) in 3215 cm^{-1}, ν (= C-H) in 3085 cm^{-1}, ν (C-H) Aromatic in 3068 cm^{-1}, ν (C-H) at 2927 cm^{-1}, ν (C≡C) in 2148 cm^{-1}, ν (C =O) at 1656 cm^{-1}, ν (C=C) in 1639 cm^{-1}, ν (C=N) in 1608 cm^{-1}, ν (C=C) aromatic in 1548 cm^{-1}; ^{1}H NMR ($CDCl_3$) : δ = 2.27 ppm. (1H, s, ≡CH), δ. 4.12 ppm. (2H, d, N-CH_2), δ = 4.79 ppm. (2H, S, S-CH_2), δ 5.29 ppm. (2H, d, =CH_2), δ = 5.91 ppm. (1H, m, =CH), δ = 7.59-8.23 ppm. (4H, m, H aromatic); ^{13}C NMR ($CDCl_3$): δ = 20.89 ppm. (=CH), δ = 46.28 ppm (N-CH_2), δ = 71.69 ppm. (≡CH), δ = 78.33 ppm. (≡C-), δ = 118.8 ppm. (=CH_2), δ = 126.04-147.27 ppm. (C Aromatic), δ = 134.47 ppm. (S-CH_2), δ 154.67 ppm. (C=N), δ = 161.41 ppm. (C=O) as shown in Figs. 3-5.

Quantum Chemical Calculations

Using density functional theory (DFT) and three-parameter replacement functional of the Lee-Yang-Parr

nonlocal correlation functional (B3LYP) with the 6-31G(d,p) basis set as implemented in the Gaussian 03 software suite, complete geometrical optimizations of the examined compounds were carried out [33]. The energies of the highest occupied and lowest unoccupied molecular orbitals (E_{HOMO} and E_{LUMO}, respectively), the molecular surface area, the binding energy, global hardness (η), the energy gap (ΔE), global softness (σ), absolute electronegativity (χ), the dipole moment (μ) and the fraction of electrons transferred from the inhibitor molecule to the metal surface (ΔN) were calculated. The optimized structures for the three compounds are shown in Fig. 6. The investigation is carried out by computations of chemical quantum structures utilizing the programs Gaussian 03W and Gaussian View 03 set. The molecular structure of inhibitors and their activity, including corrosion inhibition, are being investigated.

According to Koopman's theorem [34], energies orbitals of HOMO and LUMO for the molecules are relating to (A) electron affinity, and (I) ionization potential, continually, using the dealings:

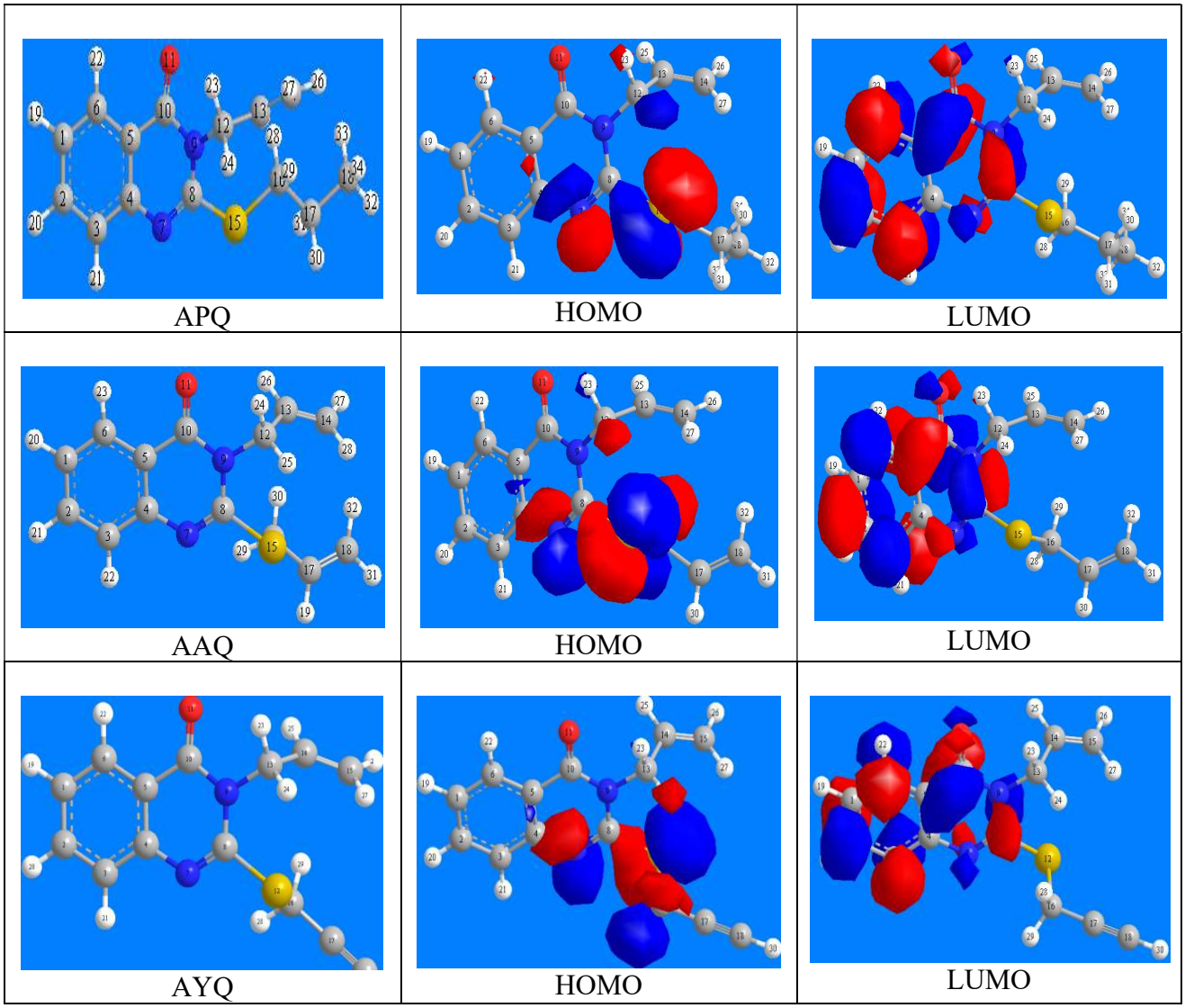

Fig. 6. The optimized geometry (E_{HOMO}) and (E_{LUMO}) of three organic compounds (corrosion inhibitors) by the B3LYP/6-31G method.

$$I = -E_{HOMO} \quad (1)$$

$$A = -E_{LUMO} \quad (2)$$

$$X = (I + A)/2 \quad (3)$$

$$\eta = (I - A)/2 \quad (4)$$

Where X is the (infinite) electronegativity, and (η) is absolute hardness for molecules inhibitors were granted using Eqs. (3) and (4) [35].

$$\sigma = 1/\eta \quad (5)$$

Global softness σ, definite as Eq. (5) [36].

$$\Delta N = [X_{Fe} - X_{inh}]/[2(\eta_{Fe} + \eta_{inhi.})] \quad (6)$$

Where $X_{Fe} = 7$, $\eta_{Fe} = 0$, and (ΔN) is the number of electrons that transferred from molecules to the surface of the metal was computed and it was found in good agreement with Pearson [37,38], as illustrated in Eq. (6). All computations were accomplished at geometry in the ground state.

RESULT AND DISCUSSION

Chemical Synthesis of Three Corrosion Inhibitors

By substituting a thiocyanate group for the chlorine atom in the molecule allyl bromide, followed by a cyclization reaction with anthranilic acid in a one-pot reaction (Fig. 2), the product (3-allyl-2-mercapto quinazoline-4(3H)-one) was synthesized (1). The absence of the carboxylic acid group and amine group is an indication that the reaction was successfully completed and appearing of new functional groups, such as (SH) and (=C-H), were identified *via* infrared spectroscopy: ν = (= C-H) in 3045 cm^{-1}, ν = (S-H) in 2488 cm^{-1}, ν. Is (C=C) in 1622 cm^{-1} and NMR spectroscopy as follows, ^{1}H NMR: δ = 1.6 ppm. (1H, s, SH), δ = 5.21,5.23 ppm. (2H, d, $=CH_2$), δ. 5.99 ppm (1 H, m, = CH-) and ^{13}C NMR: δ = 118.8 ppm. ($=CH_2$), δ = 135.54 ppm (CH=). Additionally, the molecule (3-allyl-2-mercapto quinazoline-4(3H)-one) was electrophilically substituted with propyl chloride, allyl bromide, and prop-2-yn-1-yl chloride, resulting in the preparation of various derivatives (APQ), (AAQ), and (AYQ), respectively. The following observations were made regarding the (SH) group's removal and the emergence of new groups in the FTIR and NMR spectra: FTIR: ν (C-H) in 2968 cm^{-1}, ^{1}H NMR: δ = 1.08 ppm. (3H, t, CH_3) ^{13}C NMR: δ = 13.51 ppm. (CH_3) for (APQ), ^{1}H NMR: δ = 3.97 ppm. (2H, d, S-CH_2), ^{13}C NMR: δ = 132.59 ppm. (S-CH_2) for (AAQ), FTIR: ν (≡C-H), ^{1}H NMR: δ = 2.06 ppm. (1H, s, ≡CH) ^{13}C NMR: δ 71.69 ppm. (≡CH) for (AYQ).

Quantum Chemical Calculations

The structural and electrical characteristics involved in the methods by which inhibitor molecules adhere to the surface of a metal are studied using quantum chemical simulations. According to recent research, these calculations can offer crucial insights for a deeper comprehension of the inhibition process [39]. Consequently, geometric optimizations and frontier orbitals (LUMO and HOMO) computations were performed in order to acquire a clearer description of the molecular orbitals connected with the inhibitory potential. The computed quantum chemical parameters, such as the HOMO and LUMO energies (E_{HOMO} and E_{LUMO}, respectively), the orbital energy gap (ΔE), global hardness (η), the energy gap (ΔE), global softness (σ), absolute electronegativity (χ), the dipole moment (μ) and the fraction of electrons transferred from the inhibitor molecule to the metal surface (ΔN) and the ionization potential, are presented in Table. The optimized geometry, HOMO and LUMO plots for APQ, AYQ, and AAQ in their neutral forms are shown in Fig. 2. To explore the changes in structure brought on by the different types of bonds (-CH_2-CH_3, -CH=CH_2, and -CCH) of inhibitors, calculations of DFT and relations were completed for three inhibitors, APQ, AAQ, and AYQ. The findings are shown in (Table 1) and illustrated in (Fig. 2) The electron-donating ability of inhibitory efficiency often increases with increasing E_{HOMO} value, as shown by values of E_{HOMO}. High values of E_{HOMO} demonstrate that molecules have the propensity to provide electrons to metal LUMO orbitals with low-energy unoccupied orbitals [40]. The increase in the value of E_{HOMO} makes adsorption and corrosion inhibition possible. E_{LUMO} demonstrates the ability of molecules to receive electrons; with low values, increased adsorption capacity and suitable

corrosion inhibition may be anticipated [41]. Another important descriptor that should be suggested is the energy gap (ΔE) between the HOMO and LUMO levels of the investigated inhibitors, where $\Delta E = E_{LUMO} - E_{HOMO}$. Strong values of E_{gap} indicate that it will be simpler to remove one electron from the HOMO orbital and place it in the LUMO orbital, which might result in a strong inhibitory efficiency. Elevated values of E_{gap} imply a high level of electronic stability to produce low activity. When E_{gap} values were analyzed and measured, the results showed that the compound AYQ had a small E gap of 4.999 eV. As a result, when AYQ was compared to APQ and AAQ, its high reactivity allowed it to be easily adsorbed onto the surface of carbon steel, boosting its inhibitive efficiency. The diagrams for the energy gap ΔE frontier molecular orbitals for the investigated inhibitors to their estimation are given in (Fig. 7). This coefficient is a measure of the stability of the inhibitor on the metal surface. The dipole moment is a polarity parameter for polar covalent bonds. It is seen, for instance, in the space between two bound atoms and the result of a charge on particular atoms [41]. Only the overall polarity of molecules is inverted by the whole dipole moment. When we compare the compounds listed in Table 1 to those included in the theoretical research, the computation shows that compound AYQ has a higher value of dipole moment

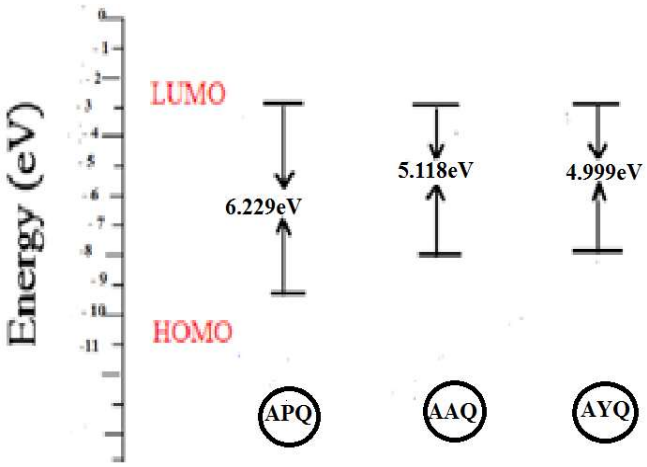

Fig. 7. Relationship diagrammatic of HOMO and LUMO orbitals for studied corrosion inhibitors with the computed ΔE_{gap} (eV).

(6.713 debye) than the obtained coefficient between AAQ and APQ (6.113 and 5.392 debye). In fact, as the dipole moment is increased, the inhibition efficiency grows. Hardness (η) and softness (σ) are two of the estimated parameters for the quantum chemical investigation. According to our theoretical findings, AYQ is significantly softer than other compounds while having a low value for

Table 1. The Parameters Used in the Chemical Quantum Calculations for the Corrosion Inhibitors which Acquired at B3LYP/6-31 Method with DFT

Quantum Chemical properties	$C_{14}H_{16}N_2OS$ (APQ)	$C_{14}H_{14}N_2OS$ (AAQ)	$C_{14}H_{12}N_2OS$ (AYQ)
E_{HOMO} (eV)	-9.129	-8.018	-7.904
E_{LUMO} (eV)	-2.900	-2.900	-2.905
ΔE(L-H) (eV)	6.229	5.118	4.999
μ (debye)	5.392	6.113	6.713
$I = -E_{HOMO}$ (eV)	9.129	8.018	7.904
$A = -E_{LUMO}$ (eV)	2.900	2.900	2.905
$X = (I + A)/2$ (eV)	6.015	5.459	5.405
$\eta = (I - A)/2$ (eV)	3.115	2.559	2.499
$\sigma = 1/\eta$	0.321	0.391	0.400
$\Delta N = (X_{Fe} - X_{inh})/2(\eta_{Fe} + \eta_{inh})$	0.158	0.301	0.319
E_T (Kcal mol^{-1})	2.875	18.740	18.164
E (RB+HF-LYP) a.u.	-1125.757	-1124.564	-1104.907

hardness. We may infer that AYQ will be tougher to adsorb than APQ and AAQ to the metal's surface. The efficacy of inhibition will flow according to the connection C≡C > C=C > C-C.

A full explanation of the contribution of electrons during a series of inhibitors is provided by the N number of transferred electrons. According to Lukovits' research [43], if $\Delta N < 3.6$, the inhibition effectiveness increased along with the capacity to donate electrons at the carbon steel/electrolyte contact. The Total Negative Charges (TNC) of AYQ are maximal compared to those of AAQ and APQ, respectively, and as a result, AYQ will exhibit better adsorption onto the surface of Carbon steel, thereby increasing its inhibition efficiency. The taken values of ΔN registered in (Table 1) are all below 3.6, and results demonstrate that substitution is acceptable given these results. We can easily observe the establishing impact of the solvent in a significant decrease of the total Energy (ET) values of the three inhibitors from calculated findings in the acid-aqueous phase (Table 1). We may thus assume that AYQ will have a stronger adsorption force than APQ and AAQ onto the metal surface. On the surface of carbon steel, the flowing relation C≡C > C=C > C-C will govern the inhibition efficiency and should lead to improved inhibition efficiency.

CONCLUSION

On some derivatives of the 2-mercapto-quinazolinone class of corrosion inhibitors in acid media, quantum chemical calculations by DFT calculations using the B3LYP/6-31G method have been conducted to investigate their geometric and electronic properties in an effort to highlight the reactivity centers of inhibitors with various types of bonds (-CH_2-CH_3, -CH=CH_2, and -CCH). A maximum inhibitory efficiency may be explained by the calculated quantum chemical parameters for HOMO, LUMO, ΔE_{gap}, Dipole moment, Hardness (η), Softness (σ), and ΔN, which is a percentage of electrons transported, and they show a perfect relationship on efficiency for inhibiting corrosion. Therefore, the structure of the examined derivatives may be related to the inhibition efficiency for the considered derivatives. Calculations revealed that the derivatives are corrosion inhibitors when we compared the compounds with each other (AYQ >AAQ >APQ).

REFERENCES

[1] Yadav, M.; Kumar, S.; Bahadur, I.; Ramjugernath, D., Corrosion inhibitive effect of synthesized thiourea derivatives on mild steel in a 15% HCl solution, *Int. J. Electrochem. Sci,* **2014**, *9*, 6529-6550, DOI: 10.1016/ j.nano.2014. 19224ccea8.

[2] Yadav, M.; Sharma, D.; Kumar, S.; Bahadur, I.; Ebenso, E., Electrochemical and theoretical studies on amino phosphonates as efficient corrosion inhibitor for N80 steel in hydrochloric acid solution, *Int. J. Electrochem. Sci,* **2014**, *9*, 6580-6593, DOI: 10.1016/j.nano.2014. 91106580.

[3] Yadav, M.; Behera, D.; Sharma, U., Nontoxic corrosion inhibitors for N80 steel in hydrochloric acid, *Arab. J. Chem.,* **2016**, *9*, S1487-S1495, DOI: 10.1016/ j.arabjc.2012.03.011.

[4] Al-Jeilawi, O. H. R.; Al-Yassiri, H., Synthesis, Characterization and Quantum Mechanical Study of Some New 2-benzylidenehydrazinecarbothioamide Derivatives as Corrosion Inhibitors for Carbon/mild Steel in Acidic Medium, *Iraqi J. Sci,* **2015**, *56*, 1-11, DOI: 10.1016/c1e809f01345f1ab.

[5] Yadav, M.; Behera, D.; Sharma, U., Corrosion protection of N80 steel in hydrochloric acid by substituted amino acids, *Corros. Eng. Sci. Technol,* **2013**, *48*, 19-27, DOI: 10.1179/1743278212Y.0000000047.

[6] Al-Sultani, K. T. A.; Al-Majidi, S. M. H.; Al-Jeilawi, O. H. R., Synthesis, Identification and Evaluation Biological Activity for Some New Triazole, Triazoline and Tetrazoline Derivatives From 2-Mercapto-3-phenyl-4 (3H) Quinazolinone, *Iraqi J. Sci.,* **2016**, *57*, 295-308, DOI: 10.1178/ c1e809f01345f1edf.

[7] Al-Zahra, A.; Al-Ani, H. N.; Al-jeilawi, O. H. R., Understanding of benzimidazole based ionic liquid as an efficient corrosion inhibitor for carbon steel: Experimental and theoretical studies, *J. Mol. Liq.*, **2022**, *358*, 119204-119214, DOI: 10.1016/ j.molliq.2022.119204.

[8] Radhi, A. H.; Du, E. A. B.; Khazaal, F. A.; Abbas, Z. M.; Aljelawi, O. H.; Hamadan, S. D.; Almashhadani, H. A.; Kadhim, M. M., HOMO-LUMO energies and geometrical structures effecton corrosion inhibition for organic compounds predict by DFT and PM3 methods,

Neuro Quantology. **2020**, *18*, 37-49, DOI: 10.14704/nq.2020.18.1.NQ20105.

[9] Banerjee, S.; Srivastava, V.; Singh, M. M., Chemically modified natural polysaccharide as green corrosion inhibitor for mild steel in acidic medium, *Corros Sci.,* **2012**, *59*, 35-41, DOI: 10.1016/j.corsci.2012.02.009.

[10] Mourya, P.; Banerjee, S.; Singh, M. M., Corrosion inhibition of mild steel in acidic solution by Tagetes erecta (Marigold flower) extract as a green inhibitor, *Corros Sci.,* **2014**, *85*, 352-363, DOI: 10.1016/ j.corsci.2014.04.036.

[11] Singh, P.; Quraishi, M. A., Corrosion inhibition of mild steel using Novel Bis Schiff's Bases as corrosion inhibitors: Electrochemical and Surface measurement, *Measurement.* **2016**, *86*, 114-124, DOI: 10.1016/ j.measurement.2016.02.052.

[12] Ashassi-Sorkhabi, H.; Shaabani, B.; Seifzadeh, D., Effect of some pyrimidinic Shciff bases on the corrosion of mild steel in hydrochloric acid solution, *Electrochim. Acta,* **2005**, *50*, 3446-3452, DOI: 10.1016/j.electacta.2004.12.019.

[13] Zhang, Q. B.; Hua, Y. X., Corrosion inhibition of mild steel by alkylimidazolium ionic liquids in hydrochloric acid, *Electrochim. Acta,* **2009**, *54*, 1881-1887, DOI: 10.1016/j.electacta.2008.10.025.

[14] Tamil Selvi, S.; Raman, V.; Rajendran, N., Corrosion inhibition of mild steel by benzotriazole derivatives in acidic medium, *J. Appl. Electrochem.,* **2003**, *33*, 1175-1182, DOI: 10.1023/B:JACH.0000003852.38068.3f.

[15] Solmaz, R.; Kardaş, G.; Çulha, M.; Yazıcı, B.; Erbil, M., Investigation of adsorption and inhibitive effect of 2-mercaptothiazoline on corrosion of mild steel in hydrochloric acid media, *Electrochim. Acta,* **2008**, *53*, 5941-5952, DOI: 10.1016/j.electacta.2008.03.055.

[16] Fouda, A. S.; Ismail, M. A.; Al-Khamri, A. A.; Abousalem, A. S., Experimental, quantum chemical and molecular simulation studies on the action of arylthiophene derivatives as acid corrosion inhibitors, *J. Mol. Liq.,* **2019**, *290*, 111178, DOI: 10.1016/ j.molliq.2019.111178.

[17] Al-tamimy, H. M. M.; Al-Majidi, S. M. H., Synthesis and Identification of 2-Pentadecyl-Quinazolinylthiourea (PQT) As Corrosion Inhibitor for Carbon Steel in Acidic Solution, *IOSR-JAC,* **2016**, *9*, 36-44, DOI: 10.9790/5736-0908023644.

[18] Hashim, N. Z. N.; Kassim, K.; Zaki, H. M.; Alharthi, A. I.; Embong, Z., XPS and DFT investigations of corrosion inhibition of substituted benzylidene Schiff bases on mild steel in hydrochloric acid, *Appl. Surf. Sci.,* **2019**, *476*, 861-877, DOI: 10.1016/ j.apsusc.2019.01.149.

[19] Rbaa, M.; Galai, M.; Benhiba, F.; Obot, I. B.; Oudda, H.; Ebn Touhami, M.; Lakhrissi, B.; Zarrouk, A., Synthesis and investigation of quinazoline derivatives based on 8-hydroxyquinoline as corrosion inhibitors for mild steel in acidic environment: experimental and theoretical studies, *Ionics.* **2019**, *25*, 3473-3491, DOI: 10.1007/s11581-018-2817-7.

[20] Chaouiki, A.; Lgaz, H.; Zehra, S.; Salghi, R.; Chung, I.-M.; El Aoufir, Y.; Bhat, K. S.; Ali, I. H.; Gaonkar, S. L.; Khan, M. I., Exploring deep insights into the interaction mechanism of a quinazoline derivative with mild steel in HCl: electrochemical, DFT, and molecular dynamic simulation studies, *J. Adhes Sci. Technol.,* **2019**, *33*, 921-944, DOI: 10.1080/ 01694243.2018.1554764.

[21] Khudhair, A. K.; Mustafa, A. M.; Hanoon, M. M.; Al-Amiery, A.; Shaker, L. M.; Gazz, T.; Mohamad, A. B.; Kadhum, A. H.; Takriff, M. S., Experimental and theoretical investigation on the corrosion inhibitor potential of N-MEH for mild steel in HCl, *PCCC,* **2022**, *15*, 111-122, DOI: 10.1080/154794243.2022.16bc.

[22] Öztürk, S., Synthesis of quinazoline derivative di-cationic surfactants and their corrosion protection of mild steel in acidic media, *Russ. J. Org. Chem.,* **2019**, *55*, 245-249, DOI: 10.1134/S1070428019020179.

[23] Majeed, M. N.; Yousif, Q. A.; Bedair, M. A., Study of the Corrosion of Nickel-Chromium Alloy in an Acidic Solution Protected by Nickel Nanoparticles, *ACS Omega*, **2022**, *7*, 29850-29857, DOI: 10.1021/ acsomega.2c02679.

[24] El-Sabbah, M. M. B.; Bedair, M. A.; Abbas, M. A.; Fahmy, A.; Hassaballa, S.; Moustafa, A. A., Synergistic Effect between Natural Honey and 0.1 M KI as Green Corrosion Inhibitor for Steel in Acid Medium, *Z. Phys. Chem.*, **2019**, *233*, 2018-1208, DOI: 10.1515/zpch-2018-1208.

[25] Abbas, M. A.; Arafa, E. I.; Bedair, M. A.; Ismail, A. S.;

El-Azabawy, O. E., Synthesis, Characterization, Thermodynamic Analysis and Quantum Chemical Approach of Branched N, N′-Bis(p-Hydroxybenzoyl)-Based Propanediamine and Triethylenetetramine for Carbon Steel Corrosion Inhibition in Hydrochloric Acid Medium, *Arab. J. Sci. Eng.*, **2022**, *48*, 7463-7484, DOI: 10.1007/s13369-022-07520-y.

[26] Bedair, M. A.; Abuelela, A. M.; Eliwa, E. M., Ethyl Ester/Acyl Hydrazide-Based Aromatic Sulfonamides: Facile Synthesis, Structural Characterization, Electrochemical Measurements and Theoretical Studies as Effective Corrosion Inhibitors for Mild Steel in 1.0 M HCl, *RSC Adv.*, **2023**, *13.1*, 186-211, DOI: 10.1039/D2RA05939H.

[27] Bedair, M. A.; Elaryian, H. M.; Ehab S. G.; Alshareef, M., Bedair, A. H.; Rabab M. A., Insights into the Adsorption and Corrosion Inhibition Properties of Newly Synthesized Diazinyl Derivatives for Mild Steel in Hydrochloric Acid: Synthesis, Electrochemical, SRB Biological Resistivity and Quantum Chemical Calculations, *RSC Adv.*, **2023**, *13.1*, 478-98, DOI: 10.1039/D2RA06574F.

[28] Bedair, M. A.; Elaryian, H. M.; Bedair, A. H.; Rabab M. A.; Fouda, A. S., Novel Coumarin-Buta-1,3-Diene Conjugated Donor-Acceptor Systems as Corrosion Inhibitors for Mild Steel in 1.0 M HCl: Synthesis, Electrochemical, Computational and SRB Biological Resistivity, *Inorg. Chem. Commun.*, **202**3, *148*, 110304, DOI: 10.1016/j.inoche.2022.110304.

[29] Saad. M.; Bedair, M. A.; Alosaimi, E. H.; Younes, A. A. O.; Abuelela, A. M., Effective Corrosion Inhibition of Mild Steel in Hydrochloric Acid by Newly Synthesized Schiff Base Nano Co(<scp>ii</Scp>) and Cr(<scp>iii</Scp>) Complexes: Spectral, Thermal, Electrochemical and DFT (FMO, NBO) Studies, *RSC Adv.*, **2022**, *12.50*, 32488-507, DOI: 10.1039/D2RA06571A.

[30] Verma, C.; Olasunkanmi, L. O.; Bahadur, I.; Lgaz, H.; Quraishi, M. A.; Haque, J.; Sherif, E.-S. M.; Ebenso, E. E., Experimental, density functional theory and molecular dynamics supported adsorption behavior of environmental benign imidazolium based ionic liquids on mild steel surface in acidic medium, *J. Mol. Liq.,* **2019**, *273*, 1-15, DOI: 10.1016/j.molliq.2018.09.139.

[31] Quartarone, G.; Battilana, M.; Bonaldo, L.; Tortato, T., Investigation of the inhibition effect of indole-3-carboxylic acid on the copper corrosion in 0.5 M H_2SO_4, *Corros Sci.,* **2008**, *50*, 3467-3474, DOI: 10.1016/j.corsci.2008.09.032.

[32] Alafeefy, A. M., Some new quinazolin-4(3H)-one derivatives, synthesis and antitumor activity, *J. Saudi Chem. Soc.*, **2011**, *15*, 337-343, DOI: org/10.1016/j.jscs.2011.06.019.

[33] Azuah, R. T.; Kneller, L. R.; Qiu, Y.; Tregenna-Piggott, P. L. W.; Brown, C. M.; Copley, J. R. D.; Dimeo, R. M., DAVE: A comprehensive software suite for the reduction, visualization, and analysis of low energy neutron spectroscopic data, *J. Res. Nat.l Inst.,* **2009**, *114*, 341, DOI: 10.6028/jres.114.025.

[34] Richards, W. G., The use of Koopmans' Theorem in the interpretation of photoelectron spectra, *IJMS,* **1969**, *2*, 419-424, DOI: 10.1016/0020-7381(69)80040-9.

[35] Ebenso, E. E.; Isabirye, D. A.; Eddy, N. O., Adsorption and quantum chemical studies on the inhibition potentials of some thiosemicarbazides for the corrosion of mild steel in acidic medium, *Int. J. Mol. Sci.,* **2010**, *11*, 2473-2498, DOI: 10.3390/ijms11062473.

[36] Udhayakala, P.; Rajendiran, T. V.; Gunasekaran, S., Theoretical evaluation on the efficiencies of some Flavonoids as corrosion inhibitors on Copper, *JCBPS,* **2012**, *2*, 1151, DOI: 10.1016/j.molstruc.2020.129416.

[37] Rauk, A., Orbital Interaction Theory of Organic Chemistry, John Wiley & Sons, **2004**, 210.

[38] Carlson, T. A.; Nestor Jr, C. W.; Wasserman, N.; McDowell, J. D., Calculated ionization potentials for multiply charged ions, *At. Data Nucl. Data Tables,* **1970**, *2*, 63-99, DOI: 10.1016/S0092-640X(70)80005-5.

[39] Bentiss, F.; Lebrini, M.; Lagrenée, M., Thermodynamic characterization of metal dissolution and inhibitor adsorption processes in mild steel/2,5-bis (n-thienyl)-1, 3, 4-thiadiazoles/hydrochloric acid system, *Corros Sci.,* **2005**, *47*, 2915-2931, DOI: 10.1016/j.corsci.2005.05.034.

[40] Obi-Egbedi, N. O.; Obot, I. B.; El-Khaiary, M. I.; Umoren, S. A.; Ebenso, E. E., Computational simulation and statistical analysis on the relationship between corrosion inhibition efficiency and molecular

structure of some phenanthroline derivatives on mild steel surface, *Int. J. Electrochem. Sci.,* **2011**, *6*, 5649-5675, DOI: 10.1016/j.apsusc.2019.04.125.

[41] Özcan, M.; Solmaz, R.; Kardaş, G.; Dehri, İ., Adsorption properties of barbiturates as green corrosion inhibitors on mild steel in phosphoric acid, *Colloids Surf., A Physicochem. Eng. Asp,* **2008**, *325*, 57-63, DOI: 10.1016/j.colsurfa.2008.04.031.

[42] Kikuchi, O., Systematic QSAR procedures with quantum chemical descriptors, *QSAR,* **1987**, *6*, 179-184, DOI: 10.1002/qsar.19870060406.

[43] Lukovits, I.; Kalman, E.; Zucchi, F., Corrosion inhibitors-correlation between electronic structure and efficiency, *Corrosion.* **2001**, *57*, 3-8, DOI: 10.5006/1.3290328.